

# Numerical Optimization and CW Measurements of SOI Waveguides for Ultra-Broadband C-to-O-Band Conversion

Tasnad Kernetzky<sup>(1)</sup>, Gregor Ronniger<sup>(2, 3)</sup>, Ulrike Höfler<sup>(1)</sup>, L. Zimmermann<sup>(2, 3)</sup>, N. Hanik<sup>(1)</sup>

<sup>(1)</sup> Technical University of Munich (TUM), Arcisstraße 21, 80333 München, Germany

<sup>(2)</sup> Technische Universität Berlin (TUB), Einsteinufer 25, 10587 Berlin, Germany

<sup>(3)</sup> IHP GmbH, Im Technologiepark 25, 15236 Frankfurt (Oder), Germany

[tasnad@tum.de](mailto:tasnad@tum.de), [g.ronniger@tu-berlin.de](mailto:g.ronniger@tu-berlin.de)

**Abstract** We analyze silicon-on-insulator waveguides, suitable for ultra-broadband inter-modal four-wave mixing-based all-optical wavelength conversion. We show numerical evaluations of waveguide modes and dispersion, and optimize phase matching. We finally present measurements of linear insertion loss and mode coupling, dispersion and four-wave mixing conversion efficiency.

## Introduction

Data transmission over the C band of optical fibers is approaching the nonlinear Shannon achievability bound<sup>[1]</sup>, and novel approaches are being developed to circumvent it. One class of approaches is mitigating fiber nonlinearity to be able to increase transmit power and therefore the signal to noise ratio. In this category, one can find digital back propagation<sup>[2]</sup>, nonlinear Fourier transform methods<sup>[3]</sup> and optical phase conjugation (OPC)<sup>[4]</sup>. A second category are space-division multiplexed techniques, i.e., transmission over multicore fibers, higher order modes of multi-mode fibers or a combination of both<sup>[5]</sup>. A third category is extending wavelength-division multiplexing beyond the C band<sup>[6]</sup>. For the latter category, all-optical wavelength converters (AOWCs) can be utilized to multiplex signals across optical bands and still use off-the-shelf C-band equipment. Wavelength conversion (WLC) is also investigated for intra-datacenter interconnects<sup>[7]</sup>. All-optical conversion does not require electrical-optical-electrical conversion, is modulation format agnostic and hence very efficient and flexible.

In this work we analyze silicon on insulator (SOI) waveguides for all-optical signal processing, which in principle covers AOWCs and OPC. We concentrate on WLC from the C to the O band as an extreme example here. We report our phase matching optimization (i.e., dispersion engineering) and continuous wave (CW) measurements of a waveguide we manufactured. We designed our waveguide to support multiple modes, providing us a further degree of freedom for phase matching (PM). This enables us to over-

come the large wavelength difference from the C to the O band using inter-modal four-wave mixing (FWM).

SOI-based AOWCs have been demonstrated in single-<sup>[8],[9]</sup> and multi-mode<sup>[10],[11]</sup> operation. Here we demonstrate that efficient, ultra-broadband operation is possible, even without having to change pump laser wavelengths. We demonstrate this by converting the whole wavelength region of the C band.

## Background and Simulations

The FWM-based all-optical signal processing we are interested in is based on exploiting material nonlinearity by launching two strong pump lasers together with a signal into two waveguide modes of a highly nonlinear medium. The waves will coherently interact and generate an idler with the desired properties, i.e., conjugated phase and/or shifted wavelength. Figure 1 sketches the experimental setup.

SOI waveguides are a very good choice as nonlinear medium. On the one hand, the large refractive index difference between silicon and silica allows for very small cross sections in the sub micrometer range – enabling integration of the devices together with BiCMOS technology. On the other hand, the nonlinearity coefficient is much larger compared to, e.g., highly nonlinear fibers,

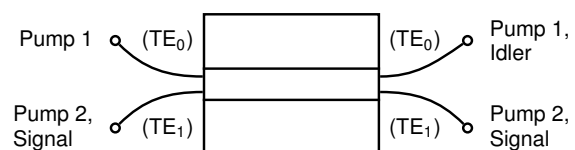


**Fig. 1:** Working principle of inter-modal FWM-based all-optical signal processing: three light waves enter the highly nonlinear waveguide (modes  $TE_0$  and  $TE_1$  in the example) and generate the FWM idler.

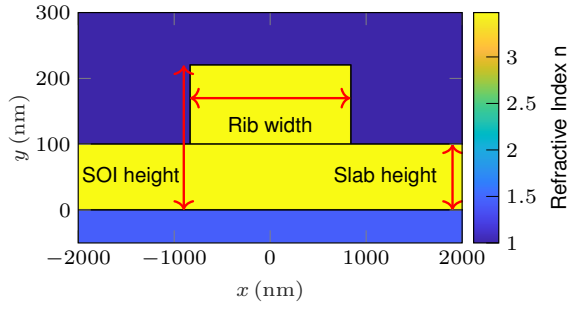


**Fig. 2:** Dimensions and refractive index of the SOI waveguide.

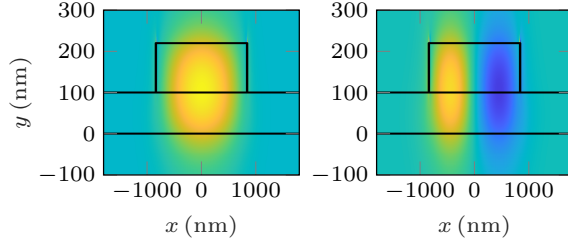
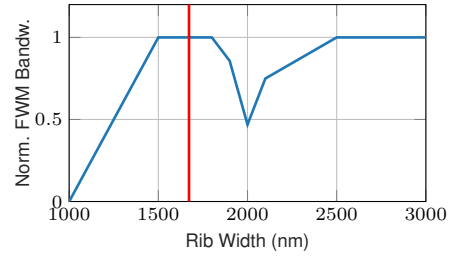


**Fig. 3:** Transversal Electrical field distribution of waveguide modes  $TE_0$  and  $TE_1$  (x components).

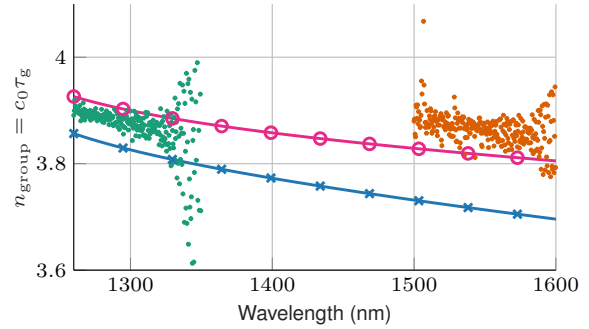
reducing device length from hundreds of meters to few centimeters. Figure 2 shows the waveguide we present in this paper – with rib width 1672 nm, slab height 100 nm and SOI height 220 nm. This device is from the second generation of chips we manufactured, for the first generation, see<sup>[12]</sup>. In comparison, this waveguide is optimized for C-to-O-band conversion and has greatly reduced linear crosstalk (XT).

Figure 3 shows the two lowest-order waveguide mode fields  $TE_0$  and  $TE_1$ , computed with a finite-difference method solver. They resemble the  $LP_{01}$  and  $LP_{11}$  modes of a multi-mode fiber, except for the smaller size and much narrower vertical than horizontal dimension. Furthermore, light is not well confined in the core, especially in waveguides with further reduced rib width and/or SOI height. This can lead to interesting dispersion properties one can exploit for PM<sup>[13]</sup>.

To reach our goal of finding a waveguide suitable for shifting the whole C band into the O band, we had to optimize the dimensions in Fig. 2. Since we were restricted by the etching process, we had to fix SOI height to 220 nm, slab height to 100 nm and could only optimize the rib width. We performed simulations with more parameters and assuming a less restrictive etching process in<sup>[13]</sup>. Figure 4 shows the best achievable 3 dB PM bandwidth for different rib widths, normalized to the width of the C band. The bandwidth is defined as the allowed signal wavelength range, such that input-output conversion efficiency (CE) is not reduced by more than 3 dB compared to



**Fig. 4:** (a) Normalized FWM bandwidth (fraction of the C band) for waveguides with varying rib widths. Marked is the device we present here.



**Fig. 5:** Waveguide dispersion. Blue crosses: Simulated  $TE_0$ , magenta circles: simulated  $TE_1$ , left green dot cloud: measured  $TE_0$ , right orange dot cloud: measured  $TE_1$ .

its maximum value, while keeping pump wavelengths fixed. We define CE as the ratio of idler power emitted from the device's output over signal power launched into the device input.

The simulated and measured dispersion of the two lowest-order modes are depicted in Fig. 5. Simulation and measurement match well, except for a constant offset which we attribute to measurement errors. However, a constant group index offset, as long as it is identical for both modes, does not affect PM.

From the dispersion in Fig. 5, one can already assess (see<sup>[14]</sup>) that placing a pump around 1300 nm in  $TE_0$  and signal and the other pump around 1520 nm in  $TE_1$ , should lead to a phase-matched idler around 1300 nm in  $TE_0$ . Indeed, the optimum is found to be 1304 nm for the O-band pump (pump 1) and 1546 nm for the C-band pump (pump 2). Figure 6 shows the resulting FWM efficiency w.r.t. varying signal and pump 2 wavelengths, while pump 1 is fixed at 1304 nm. FWM efficiency is defined as<sup>[15]</sup>  $\eta = (1 - \exp(-(\alpha + j\Delta\beta)L)) / ((\alpha + j\Delta\beta)L)$  with phase mismatch  $\Delta\beta$ , waveguide length  $L$  and attenuation  $\alpha$ . We depict the normalized quantity  $|\eta| / \max(|\eta|)$ . The CE is proportional to  $|\eta|^2$ . The horizontal marked region is the configuration with highest bandwidth and is shown in Fig. 7 in detail.

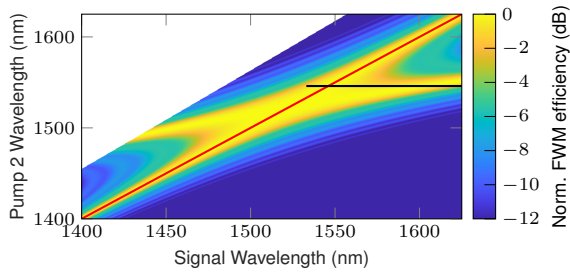


**Fig. 6:** Normalized FWM efficiency for pump 1 fixed at 1304 nm. The red diagonal line shows where signal and second pump have identical wavelengths and the horizontal line marks the region shown in Fig. 7.

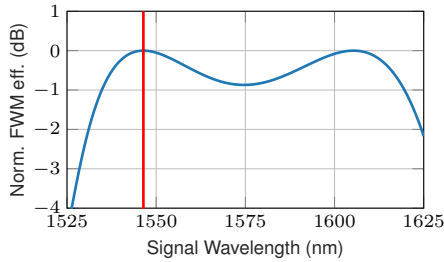


**Fig. 7:** Normalized FWM efficiency for the presented device. C-band pump wavelength is indicated in red.

## Measurements

For the presented waveguide, we performed several CW measurements. Figure 8 shows the losses from input and output grating couplers (GCs) and mode multiplexers (MUXs), with just a very short piece of waveguide connecting the ports, which we consider as back to back (B2B) case. Comparing Fig. 7 and Fig. 8, one can see that the bandwidth is currently limited by the GCs. We do not expect the MUXs to limit bandwidth.

We noticed that SOI waveguides can have severe linear XT<sup>[12]</sup>. Figure 9 shows the measured power transfer from different input to output ports of the waveguide, normalized to the B2B measurements obtained in Fig. 8. It is evident that there is still fading due to linear XT, although it is much reduced compared to our first generation of waveguides<sup>[12]</sup>. For the intended C-to-O-band operation, we expect narrow “dips” in CE of up to 10 dB due to linear XT.

Figure 10 shows the normalized FWM efficiency for varying values of signal and pump, in

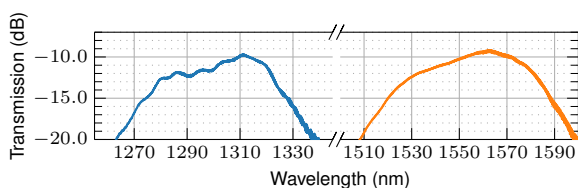


**Fig. 8:** B2B measurement of waveguide transmission with only negligible waveguide length. Measurements include grating coupler and mode multiplexer losses at both input and output. Transmission is through the TE<sub>0</sub> and TE<sub>1</sub> modes for O and C band, respectively.

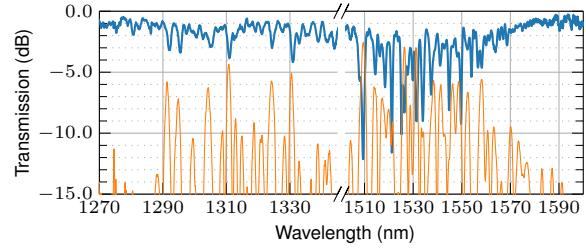


**Fig. 9:** Waveguide power transmission (upper blue lines) and linear crosstalk (lower orange lines). O band is propagating in TE<sub>0</sub> mode; C band is propagating in TE<sub>1</sub> mode.

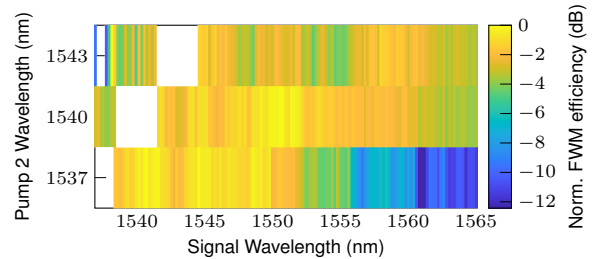


**Fig. 10:** Input-output conversion efficiency for varying signal and C-band pump wavelengths, normalized to peak efficiency for each C-band pump wavelength. O-band pump wavelength is fixed at 1300 nm

analogy to Fig. 6. Due to a slight offset between measurement and simulation, we used an O-band pump wavelength of 1300 nm to get the best measured bandwidth. Comparing the two figures, one can see that the bandwidth is smaller in Fig. 10 and we attribute the difference firstly to the limiting effect of the GCs and secondly to linear XT.

We finally conclude that the bandwidth in Fig. 10 (for pump 2 at 1540 nm) is sufficient to shift wavelengths from the whole C band to the O band and hence we confirm the ultra-broadband WLC capabilities of the presented waveguide. Verification of this performance in a system experiment is shown in another contribution to the same conference.

## Conclusions

We presented an SOI waveguide suitable for shifting wavelengths from the whole C band into the O band by FWM-based all-optical signal processing, without having to change pump laser wavelengths. We performed dispersion simulations, phase matching optimizations and CW measurements and improved the linear XT characteristics of the SOI waveguide. We expect an even better performance in next generations.

## Acknowledgments

This work was supported by the DFG projects PE 319/36-2, ZI 1283/3-2, HA 6010/6-1, ZI 1283/5-1 and FR 851/3-1.

## References

- [1] R.-J. Essiambre, G. Kramer, P. J. Winzer, G. J. Foschini, and B. Goebel, "Capacity limits of optical fiber networks", *J. Lightw. Technol.*, vol. 28, pp. 662–701, 2010, ISSN: 0733-8724, 1558-2213. DOI: 10.1109/JLT.2009.2039464.
- [2] X. Li, X. Chen, G. Goldfarb, E. Mateo, I. Kim, F. Yaman, and G. Li, "Electronic post-compensation of WDM transmission impairments using coherent detection and digital signal processing", *Opt. Express*, vol. 16, p. 880, 2008, ISSN: 1094-4087. DOI: 10.1364/OE.16.000880.
- [3] M. I. Yousefi and F. R. Kschischang, "Information transmission using the nonlinear Fourier transform, part I: Mathematical tools", *IEEE Trans. Inf. Theory*, vol. 60, pp. 4312–4328, 2014, ISSN: 0018-9448, 1557-9654. DOI: 10.1109/TIT.2014.2321143.
- [4] I. Sackey, A. Gajda, A. Peczek, E. Liebig, L. Zimmermann, K. Petermann, and C. Schubert, "1024 Tb/s wavelength conversion in a silicon waveguide with reverse-biased p-i-n junction", *Opt. Express*, vol. 25, p. 21229, 2017, ISSN: 1094-4087. DOI: 10.1364/OE.25.021229.
- [5] R. S. Luis, G. Rademacher, B. J. Puttnam, T. A. Eriksson, H. Furukawa, A. Ross-Adams, S. Gross, M. Withford, N. Riesen, Y. Sasaki, K. Saitoh, K. Aikawa, Y. Awaji, and N. Wada, "1.2 Pb/s throughput transmission using a 160 $\mu$ m cladding, 4-core, 3-mode fiber", *J. Lightw. Technol.*, vol. 37, pp. 1798–1804, 2019, ISSN: 0733-8724, 1558-2213. DOI: 10.1109/JLT.2019.2902601.
- [6] B. J. Puttnam, R. S. Luis, G. Rademacher, L. Galdino, D. Lavery, T. A. Eriksson, Y. Awaji, H. Furukawa, P. Bayvel, and N. Wada, "0.61 Pb/s S, C, and L-band transmission in a 125 $\mu$ m diameter 4-core fiber using a single wideband comb source", *J. Lightw. Technol.*, vol. 39, pp. 1027–1032, 2021, ISSN: 0733-8724, 1558-2213. DOI: 10.1109/JLT.2020.2990987.
- [7] F. Yan, W. Miao, T. Li, Y. Maeda, Z. Cao, and N. Calabretta, "Monolithically integrated wavelength converter for intra-data center routing applications", *IEEE Photon. Technol. Lett.*, vol. 28, pp. 2854–2857, 2016, ISSN: 1041-1135, 1941-0174. DOI: 10.1109/LPT.2016.2623748.
- [8] D. Wu, L. Shen, H. Ren, M. Huang, C. Lacava, J. Campling, S. Sun, T. W. Hawkins, U. J. Gibson, P. Petropoulos, J. Ballato, and A. C. Peacock, "Four-wave mixing-based wavelength conversion and parametric amplification in submicron silicon core fibers", *IEEE J. Sel. Topics Quantum Electron.*, vol. 27, pp. 1–11, 2021, ISSN: 1077-260X, 1558-4542. DOI: 10.1109/JSTQE.2020.3022100.
- [9] J. Chen and S. Gao, "Wavelength-assignable 1310/1550 nm wavelength conversion using completely phase-matched two-pump four-wave mixing in a silicon waveguide", *Opt. Commun.*, vol. 356, pp. 389–394, 2015, ISSN: 00304018. DOI: 10.1016/j.optcom.2015.08.014.
- [10] S. Signorini, M. Finazzer, M. Bernard, M. Ghulinyan, G. Pucker, and L. Pavesi, "Silicon photonics chip for inter-modal four wave mixing on a broad wavelength range", *Front. Phys.*, vol. 7, p. 128, 2019, ISSN: 2296-424X. DOI: 10.3389/fphy.2019.00128.
- [11] C. Lacava, M. Ettabib, T. D. Bucio, G. Sharp, A. Khokhar, Y. Jung, D. Richardson, P. Petropoulos, F. Gardes, M. Sorel, and F. Parmigiani, "Inter-modal wavelength conversion in silicon waveguide", in *2018 European Conference on Optical Communication (ECOC)*, Rome: IEEE, 2018, pp. 1–3, ISBN: 978-1-5386-4862-9. DOI: 10.1109/ECOC.2018.8535169.
- [12] G. Ronniger, S. Lischke, C. Mai, L. Zimmermann, and K. Petermann, "Investigation of inter-modal four wave mixing in p-i-n diode assisted SOI waveguides", in *2020 IEEE Photonics Society Summer Topicals Meeting Series (SUM)*, Cabo San Lucas, Mexico: IEEE, 2020, TuD2.3, ISBN: 978-1-72815-887-7. DOI: 10.1109/SUM48678.2020.9161068.
- [13] T. Kernetzky, Y. Jia, and N. Hanik, "Multi dimensional optimization of phase matching in multimode silicon nano-rib waveguides", in *Photonic Networks; 21st ITG-Symposium*, Leipzig, Germany, 2020, ISBN: 978-3-8007-5423-6.
- [14] R.-J. Essiambre, M. A. Mestre, R. Ryf, A. H. Gnauck, R. W. Tkach, A. R. Chraplyvy, Y. Sun, X. Jiang, and R. Lingle, "Experimental investigation of inter-modal four-wave mixing in few-mode fibers", *IEEE Photon. Technol. Lett.*, vol. 25, pp. 539–542, 2013, ISSN: 1041-1135, 1941-0174. DOI: 10.1109/LPT.2013.2242881.
- [15] K. O. Hill, D. C. Johnson, B. S. Kawasaki, and R. I. MacDonald, "CW three-wave mixing in single-mode optical fibers", *J. Appl. Phys.*, vol. 49, pp. 5098–5106, 1978, ISSN: 0021-8979, 1089-7550. DOI: 10.1063/1.324456.